基于 2,4,6-吡啶三酸配体的 Co(II)、Ni(II)配位聚合物的合成、结构和磁性分析

银秀菊[1]　廖蓓玲[1]　吴汉民[1]　庞毅林[1]　李石雄*,[1,2]

([1] 河池学院化学与生物工程学院, 宜州　546300)
([2] 华南理工大学环境与能源学院, 广州　510006)

摘要：以 2,4,6-吡啶三酸为配体, 采取水热合成的方法, 在相同温度、物质的量之比、溶剂, 不同金属盐条件下合成了{[M_3(pyta)$_2$(H$_2$O)$_8$]·4H$_2$O}$_n$(M=Co(**1**), Ni(**2**), H$_3$pyta=2,4,6-吡啶三酸)配位聚合物。X 射线单晶衍射测试分析表明 2 个配合物是异质同晶结构, 属于单斜晶系, $P2_1/c$ 空间群。磁性测试表明在配合物的中心离子 M(II)之间存在反铁磁耦合作用。

关键词：配位聚合物；2,4,6-吡啶三酸；磁性

Syntheses, Structures and Magnetic Analysis of Co(II), Ni(II) Coordination Polymers Based on Pyridine-2,4,6-tricarboxylic Acid

YIN Xiu-Ju[1]　　LIAO Bei-Ling[1]　　WU Han-Min[1]　　PANG Yi-Lin[1]　　LI Shi-Xiong*,[1,2]

([1] *College of Chemistry and Biological Engineering, Hechi University, Yizhou, Guangxi 546300, China*)
([2] *School of Environment and Energy, South China University of Technology, Guangzhou 510006, China*)

Abstract: The title coordination polymers of {[M_3(pyta)$_2$(H$_2$O)$_8$]·4H$_2$O}$_n$(M=Co(**1**), Ni(**2**)) based on H$_3$pyta (H$_3$pyta= pyridine-2,4,6-tricarboxylic acid) had been synthesized under hydrothermal synthesis conditions with same temperature, molar ratio and solvent, but different metal salts. X-ray diffraction analysis shows that these two polymers are hetero-isomorphic and belong to the monoclinic system, $P2_1/c$ space group. The magnetic investigation shows that polymers **1** and **2** exhibit a ferromagnetic coupling between M(II) ions. CCDC: 1524314, **1**; 1000880, **2**.

Keywords: coordination polymer; pyridine-2,4,6-tricarboxylic acid; magnetic

0　Introduction

Since "single-molecule magnets" (SMMs) were discovered, design and synthesis of the paramagnetic transition polymetallic cluster are attractive to researchers[1-5]. Recently many different directions have being pursued in the research field of SMMs[6-11], in which an important direction has been found that the intermolecular interaction with different correlation in the whole molecular arrangement, though very weak, can perturb the intrinsic properties of individual SMMs[12]. In our previous work[13-14], we have reported and studied antiferromagnetic(AF) coupling interaction between magnetic centers. Ligands 3-/4- pyridinecarboxylate and pyridinecarboxylate have recently been found to act as excellent building

blocks with charge and multi-connecting ability in the construction of functional coordination polymers with porosity, photolumineseent or magnetic properties[15-16]. Compared with the previously investigated pyridinecarboxylate ligands, pyridine-2,4,6-tricarboxylic acid (H$_3$pyta) have the advantages of multiple bridging moieties, which leads to a variety of connection modes with transition metal centers and provides abundant structural motifs. It can act not only as N-donors but also as O$_{carboxylate}$-donors to chelate or bridge metal ions to form coordination polymers[17], and some complexes can act as SMMs [18]. In this paper, we report Co(II) and Ni(II) polymers based on pyridine-2,4,6-tricarboxylic acid (H$_3$pyta): {[M$_3$(pyta)$_2$(H$_2$O)$_8$]·4H$_2$O}$_n$, and analyze their thermogravimetric and magnetic properties.

1 Experimental

All solvents and chemicals were commercial reagents and used without further purification. pyridine-2,4,6-tricarboxylic acid was synthesized according to the reference [17]. Elemental analyses (carbon, hydrogen, and nitrogen) were performed with a Perkin-Elmer 240 elemental analyzer. IR spectra were measured from KBr pellets on a Nicolet 5DX FTIR spectrometer. XRD was performed using Rigaku D/max 2500 X-ray diffractometer (Cu $K\alpha$ radiation, λ =0.156 04 nm, U=40 kV, I=150 mA, 2θ=5°~65°). The TGA was determined by Perkin Elmer Pyris Diamond TG-DTA. The magnetic measurements were carried out with a Quantum Design MPMS-XL7 and a PPMS-9 ACMS magnetometer.

1.1 Synthesis of {[Co$_3$(pyta)$_2$(H$_2$O)$_8$]·4H$_2$O}$_n$ (1)

CoCl$_2$·6H$_2$O(0.072 4 g,3 mmol), H$_3$ptc(0.021 1 g, 1 mmol) were mixed in 7 mL distilled H$_2$O water and 3 mL ethanol. The pH value of the solution was adjusted to 7 with 1 mol·L^{-1} NaOH, and then sealed in a 23 mL Teflon-lined stainless steel autoclave. The mixture was heated in an oven at 100 ℃ for two days , and cooled to room temperature at a rate of 10 ℃·h^{-1}. Red massive crystals of **1** were obtained. Yield: 95% (based on H$_3$ptc). Anal. Calcd. for C$_{16}$H$_{28}$Co$_3$N$_2$O$_{24}$ (%): C, 23.74; H, 3.46; N, 3.46. Found (%): C, 23.77; H, 3.40; N, 3.48. IR(cm^{-1}): 3 448s, 1622s, 1 509w, 1 444w, 1 378s, 1 312w, 1 256w,1 114w, 926w, 747m, 512m.

1.2 Synthesis of{[Ni$_3$(pyta)$_2$(H$_2$O)$_8$]·4H$_2$O}$_n$(2)

The procedures were similar to the synthesis of **1** except that the metal salts was NiCl$_2$·6H$_2$O. Green massive crystals of **2** were obtained. Yield: 86% . (based on H$_3$ptc). Anal. Calcd. for C$_{16}$H$_{28}$Ni$_3$N$_2$O$_{24}$ (%): C, 23.75; H, 3.46; N, 3.46. Found (%): C, 23.81; H, 3.41; N, 3.52. IR (cm^{-1}): 3 853m, 3 749m, 3 438s, 2 348w, 1 622s, 1 430w, 1 378s, 1 289w,1 113w, 926w, 747m, 512m.

1.3 X-ray diffraction

Single-crystal X-ray diffraction data were collected on a Agilent supernova diffractometer equipped with graphite-monochromated Mo radiation with radiation wavelength 0.071 073 nm, by using the x-scan technique. For **1** and **2**, the structures were solved by direct methods using the SHELXS-2013 [19], and refined by full-matrix least-squares on F^2 using the Olex^2 program[20]. All non-hydrogen atoms were refined anistropically. Hydrogen atoms were generated geometrically and refined isotropically with the riding mode. Crystallographic crystal data and structure processing parameters for polymers **1~2** are summarized in Table 1. Selected bond lengths and bond angles for polymers **1~2** are listed in Table 2, and hydrogen bonds for polymers **1~2** are listed in Table 3.

CCDC: 1524314, **1**; 1000880, **2**.

Table 1 Crystal data and structure parameters for polymers 1~2

Polymer	1	2
Empirical formula	C$_{16}$H$_{28}$Co$_3$N$_2$O$_{24}$	C$_{16}$H$_{28}$Ni$_3$N$_2$O$_{24}$
Formula weight	809.19	808.53
T / K	298	296
Crystal system	Monoclinic	Monoclinic
Space group	$P2_1/c$	$P2_1/c$

Continued Table 1

a / nm	0.718 0(3)	0.713 56(16)
b / nm	1.185 75(8)	1.857 4(4)
c / nm	1.083 5(5)	1.076 1(2)
β / (°)	103.880(5)	103.225(3)
V / nm³	1.402 9(10)	1.388 4(5)
D_c / (g·cm⁻³)	1.916	1.934
Z	2	2
Limiting indices	$-8 \leqslant h \leqslant 8$	$-8 \leqslant h \leqslant 8$
	$-22 \leqslant k \leqslant 22$	$-21 \leqslant k \leqslant 22$
	$-12 \leqslant l \leqslant 12$	$-12 \leqslant l \leqslant 12$
$F(000)$	822	828
θ range / (°)	2.2~25.1	2.2~25.1
S	1.00	1.00
R_{int}	0.034	0.023
Reflections, parameters, restraints	2 496, 205, 0	2 465, 205, 0
$R_1{}^*[c \geqslant 2\sigma(\text{parameters, restraints})]$	0.023	0.027
$wR_2{}^*$	0.051	0.067
μ / mm⁻¹	1.86	2.12
$(\Delta/\sigma)_{max}$	0.001	0.001
$(\Delta\rho)_{max}$, $(\Delta\rho)_{min}$ / (e·nm⁻³)	340, −530	320, −440

$^*R_1 = \sum(||F_o| |F_c||)/\sum|F_o|$, $wR_2 = [\sum(||F_o|^2|F_c||^2)^2/\sum|F_o|^2]^{1/2}$

Table 2 Selected bond lengths (nm) and bond angles (°) for polymers 1~2

1					
Co(1)-O(1)A	0.202 16(15)	Co(2)-O(5)	0.207 49(15)	Co(1)-N(1)	0.205 40(17)
Co(2)-O(5)B	0.207 49(15)	Co(1)-O(7)	0.207 60(18)	Co(2)-O(9)B	0.208 6(2)
Co(1)-O(8)	0.211 24(18)	Co(2)-O(9)	0.208 6(2)	Co(1)-O(6)	0.215 57(15)
Co(2)-O(10)B	0.210 23(19)	Co(1)-O(2)	0.226 94(16)	Co(2)-O(10)	0.210 23(19)
O(1)A-Co(1)-N(1)	176.96(6)	O(5)-Co(2)-O(5)B	180	O(1)A-Co(1)-O(7)	87.90(6)
O(5)-Co(2)-O(9)B	93.70(7)	N(1)-Co(1)-O(7)	89.24(6)	O(5)B-Co(2)-O(9)B	86.30(7)
O(1)A-Co(1)-O(8)	84.77(6)	O(5)-Co(2)-O(9)	86.30(7)	N(1)-Co(1)-O(8)	98.10(6)
O(5)B-Co(2)-O(9)	93.70(7)	O(7)-Co(1)-O(8)	172.64(6)	O(9)B-Co(2)-O(9)	180
O(1)A-Co(1)-O(6)	103.55(6)	O(5)-Co(2)-O(10)B	88.46(6)	N(1)-Co(1)-O(6)	75.51(6)
O(5)B-Co(2)-O(10)B	91.54(6)	O(7)-Co(1)-O(6)	91.83(7)	O(9)B-Co(2)-O(10)B	92.39(9)
O(8)-Co(1)-O(6)	90.50(7)	O(9)-Co(2)-O(10)B	87.61(9)	O(1)A-Co(1)-O(2)	107.43(6)
O(5)-Co(2)-O(10)	91.54(6)	N(1)-Co(1)-O(2)	73.87(6)	O(5)B-Co(2)-O(10)	88.46(6)
O(7)-Co(1)-O(2)	95.47(6)	O(9)B-Co(2)-O(10)	87.61(9)	O(8)-Co(1)-O(2)	86.16(6)
O(9)-Co(2)-O(10)	92.39(9)	O(6)-Co(1)-O(2)	148.38(5)	O(10)B-Co(2)-O(10)	180
2					
Ni(1)-N(1)	0.199 6(2)	Ni(2)-O(5)B	0.202 29(17)	Ni(1)-O(1)A	0.200 10(18)
Ni(2)-O(5)	0.202 29(17)	Ni(1)-O(7)	0.204 7(2)	Ni(2)-O(10)B	0.206 9(2)
Ni(1)-O(8)	0.205 5(2)	Ni(2)-O(10)	0.206 9(2)	Ni(1)-O(6)	0.212 39(18)
Ni(2)-O(9)	0.2075(2)	Ni(1)-O(2)	0.229 56(19)	Ni(2)-O(9)B	0.207 5(2)

Continued Table 2

N(1)-Ni(1)-O(1)A	178.12(8)	O(1)A-Ni(1)-O(8)	85.47(8)	N(1)-Ni(1)-O(7)	90.44(8)
O(7)-Ni(1)-O(8)	173.13(7)	O(1)A-Ni(1)-O(7)	87.81(8)	N(1)-Ni(1)-O(6)	78.00(8)
N(1)-Ni(1)-O(8)	96.26(8)	O(1)A-Ni(1)-O(6)	102.71(7)	O(7)-Ni(1)-O(6)	91.24(8)
O(5)-Ni(2)-O(10)	93.06(8)	O(8)-Ni(1)-O(6)	91.67(8)	O(10)B-Ni(2)-O(10)	180
N(1)-Ni(1)-O(2)	74.62(7)	O(5)B-Ni(2)-O(9)	93.62(8)	O(1)A-Ni(1)-O(2)	104.81(7)
O(5)-Ni(2)-O(9)	86.38(8)	O(7)-Ni(1)-O(2)	93.75(8)	O(10)B-Ni(2)-O(9)	87.87(12)
O(8)-Ni(1)-O(2)	86.56(8)	O(10)-Ni(2)-O(9)	92.13(12)	O(6)-Ni(1)-O(2)	152.19(7)
O(5)B-Ni(2)-O(9)B	86.38(8)	O(5)B-Ni(2)-O(5)	180	O(5)-Ni(2)-O(9)B	93.62(8)
O(5)B-Ni(2)-O(10)B	93.06(8)	O(10)B-Ni(2)-O(9)B	92.13(12)	O(5)-Ni(2)-O(10)B	86.94(8)
O(10)-Ni(2)-O(9)B	87.87(12)	O(5)B-Ni(2)-O(10)	86.94(8)	O(9)-Ni(2)-O(9)B	180

Symmetry codes: A: x, $-y+1/2$, $z+1/2$; B: $-x$, $-y+1$, $-z+1$; C: x, $-y+1/2$, $z-1/2$

Table 3　Hydrogen bonds parameters for polymers 1 and 2

D-H⋯A	d(D-H) / nm	d(H⋯A) nm	d(D⋯A) / nm	∠D-H⋯A/(°)
1				
O(8)-H(8)b⋯O(12)D	0.079	0.200	0.273 2(2)	156
O(8)-H(8)a⋯O(4)E	0.090	0.182	0.271 5(2)	172
O(7)-H(7)b⋯O(12)F	0.082	0.196	0.276 1(2)	165
O(7)-H(7)a⋯O(3)G	0.086	0.182	0.268 2(2)	175
O(9)-H(9)b⋯O(11)	0.081	0.202	0.282 6(3)	174
O(9)-H(9)a⋯O(3)H	0.087	0.182	0.267 0(2)	168
O(10)-H(10)b⋯O(8)A	0.091	0.242	0.302 2(3)	124
O(10)-H(10)a⋯O(6)	0.078	0.203	0.264 5(2)	137
O(11)-H(11)b⋯O(9)I	0.088	0.251	0.329 1(3)	148
O(11)-H(11)a⋯O(2)A	0.078	0.232	0.304 3(3)	154
O(12)-H(12)b⋯O(4)	0.079	0.194	0.272 1(2)	167
O(12)-H(12)a⋯(11)I	0.089	0.195	0.283 7(3)	173
2				
O(8)-H(8)b⋯O(12)D	0.084	0.193	2.744(3)	162
O(8)-H(8)a⋯O(4)E	0.085	0.186	2.702(3)	173
O(7)-H(7)b⋯O(12)F	0.084	0.194	2.771(3)	167
O(7)-H(7)a⋯O(3)G	0.084	0.185	2.688(3)	174
O(9)-H(9)b⋯O(11)	0.085	0.200	2.848(3)	175
O(9)-H(9)a⋯O(3)G	0.085	0.183	2.666(3)	166
O(10)-H(10)b⋯O(8)A	0.083	0.246	3.075(3)	132
O(10)-H(10)a⋯O(6)	0.085	0.196	2.653(3)	137
O(11)-H(11)b⋯O(9)H	0.083	0.244	3.172(4)	147
O(11)-H(11)a⋯O(2)I	0.084	0.221	2.994(3)	155
O(12)-H(12)b⋯O(4)	0.085	0.189	2.735(3)	170
O(12)-H(12)a⋯O(11)I	0.085	0.198	2.818(3)	169

Symmetry codes: A: x, $-y+1/2$, $z+1/2$; D: $-x$, $y-1/2$, $z+1/2$; E: $-x$, $-y+1$, $-z$; F: $-x+1$, $y-1/2$, $-z+1/2$; G: $-x+1$, $-y+1$, $-z$; H: x, y, $z+1$; I: $-x+1$, $-y+1$, $-z+1$

2　Results and discussion

2.1　Crystal structures of 1 and 2

X-ray single-crystal diffraction analysis reveals that polymers **1** and **2** crystallizes in monoclinic system, space group $P2_1/c$, they are hetero-isomorphic and two-dimensional structure polymers. The coordination environment of M(Ⅱ) in **1** and **2** is shown in Fig.1a. The asymmetric unit consists of three M(Ⅱ) ions, two pyta³⁻ ligand, eight coordinated water molecules, and four free water molecules.

There are three separate M(Ⅱ) ions and two coordination modes in the polymers. The first coordination mode is that the M(Ⅱ) ion is coordinated by one nitrogen atom(N1) and three oxygen atoms(O1, O2,O6) from pyta³⁻ ligand and two coordinated water molecules (O7,O8). The other one is that the M(Ⅱ) ion is coordinated by six oxygen atoms (O5,O5B from two different pyta³⁻ ligand and O9, O9A, O10, O10A from four coordinated water molecules). These two different M(Ⅱ) ions in **1** and **2** both are six-coordinated. For polymer **1**, the Co-O distances fall in the range of 0.202 16(15)~0.226 94(16) nm. The Co-N distance is 0.205 40(17) nm. The bond angles of N1-Co1-O2 and O10-Co2-O10B are 73.87(6)° and 180.0°, respectively. For polymer **2**, the Ni-O distances fall in the range of 0.200 10(18)~0.229 56(19) nm. The Ni-N distance is 0.199 6(2) nm. The bond angles of N1-Ni1-O2 and O9B-Ni2-O9 are 74.62(7)° and 180.0°, respectively. These bond angles and bond distances all fall in the normal ranges[17,21].
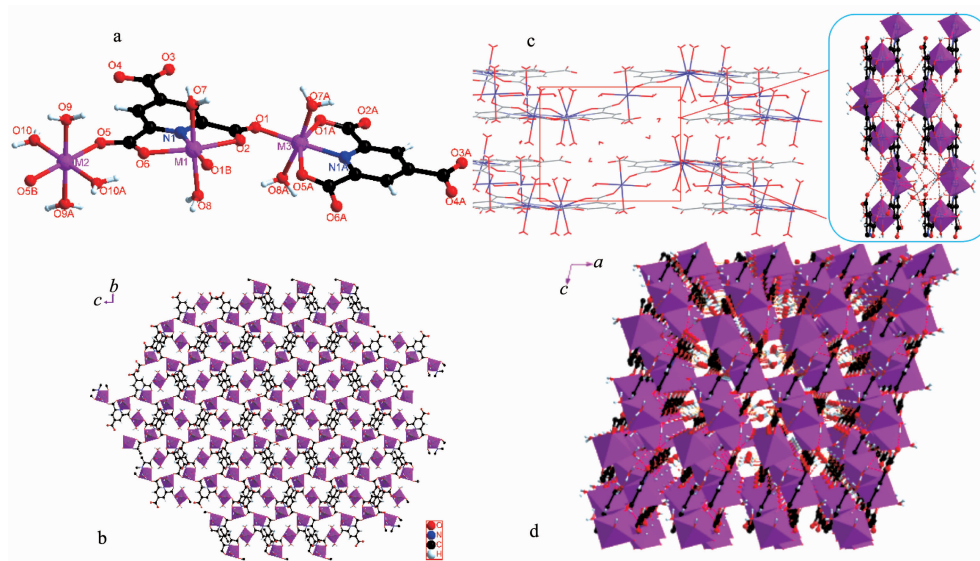
Symmetry codes: A: x, $-y+1/2$, $z+1/2$; B: $-x$, $-y+1$, $-z+1$; C: x, $-y+1/2$, $z-1/2$ in (a)

Fig.1　(a) Coordination environment of M(Ⅱ)(M=Co, Ni) ions in **1~2**; (b) 2-D network structure of polymers **1~2** viewed along a axis; (c)Hydrogen bonds in **1~2**; (d) 3D structure of **1~2** formed by hydrogen bonds viewed along b axis

In polymers **1** and **2**, the five coordination sites on the ligand all coordinate with metal ions. So, the pyta³⁻ ligand adopts a μ_5-η^1:η^2:η^2 bridging style to coordinate with M(Ⅱ) ions. Two O atoms from carboxyl of ligand coordinate with two M(Ⅱ) ions, so carboxyl adopts a μ_2-η^1:η^1 bridging style to coordinate with M(Ⅱ) ions. As the ligand adopts a μ_5-η^1:η^2:η^2 bridging style and carboxyl takes a μ_2-η^1:η^1 bridging style, the polymers **1** and **2** exhibit a very special two-

dimensional network structure along a axis (Fig.1b).

Owing to the introduction of water molecules, the crystals of polymers **1** and **2** have a large number of hydrogen bonds. The O atoms in carbonyl group on the ligand form O-H⋯O intramolecular hydrogen bonds with coordinated water molecules. The free water molecules in polymers **1** and **2** form O-H⋯O intermolecular hydrogen bonds with coordinated water molecules (Fig.1c). These hydrogen bonds finally

generate a three-dimensional network structure by bridging the two-dimensional planes with intermolecular hydrogen bonds (Fig.1d).

2.2 PXRD and thermal gravimetric analysis

In order to check the purity of polymers **1** and **2**,

powder X-ray diffraction of the as-synthesized samples was measured at room temperature. The peak positions of experimental patterns are in good agreement with the simulated ones, which clearly indicates good purity of the polymers **1** and **2**(Fig.2).
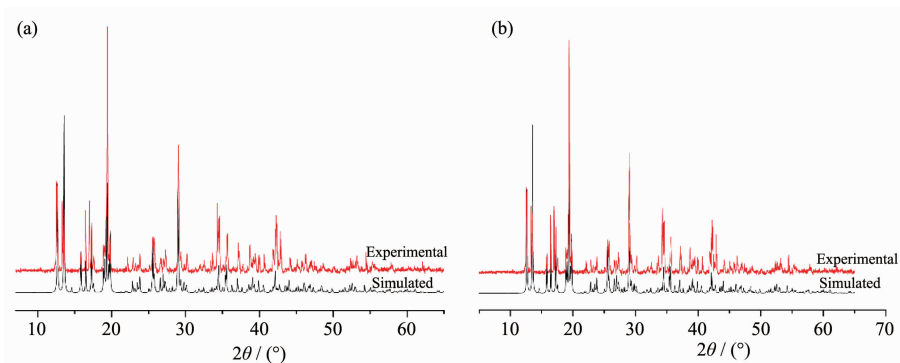

Fig.2　PXRD patterns for polymers **1**(a) and **2**(b)

The thermal stabilities of polymers **1** and **2** were tested in the range of 45~1 000 ℃ under a nitrogen atmosphere at a heating rate of 5℃·min^{-1} and TGA curves of polymers **1** and **2** were shown in Fig.3. The TGA curve of **1** show that polymer **1** first loses twelve water molecules(Obsd. 27.59%, Calcd. 26.69%) in the range of 45~236 ℃. The second weight loss is responsible for the decomposition of all organic components in the range of 236~556 ℃. The residue with weight of 31.72% might be Co_2O_3 (Calcd. 30.75%).The TGA curve of **2** show that polymer **2** first loses twelve water molecules (Obsd. 23.52%, Calcd. 23.75%) in the range of 45~123 ℃. Further weight loss is responsible for the decomposition of all organic components in the range of 123~503 ℃. The residue with weight of 28.79% might be NiO(Calcd. 27.71%).

2.4 Magnetic analysis for polymers 1~2

Co(Ⅱ) (d^7) of polymer **1** and Ni(Ⅱ) (d^8) of polymer **2** have unpaired electrons, so their magnetic properties are studied. The magnetic susceptibilities, χ_m of **1** and **2** were measured in the 2 ~300 K temperature range, and shown as plots of χ_m and $\chi_m T$ versus T in Fig.4a and Fig.4b, respectively. As shown in Fig.4a, the molar magnetic susceptibility χ_m of polymer **1** increases gradually as the temperature lowers, and more rapidly increases below 25 K, then reaches a maximum value of 2.24 cm^3·mol^{-1} at 2 K. It can be seen from the $\chi_m T$ curve that the $\chi_m T$ value is 9.56 cm^3·mol^{-1}·K at 300 K, which is significantly higher than the theoretical value 5.64 cm^3·mol^{-1}·K of the high-spin triplet Co^{2+}, indicating a great spin-orbit coupling contribution. As the decrease of temperature,
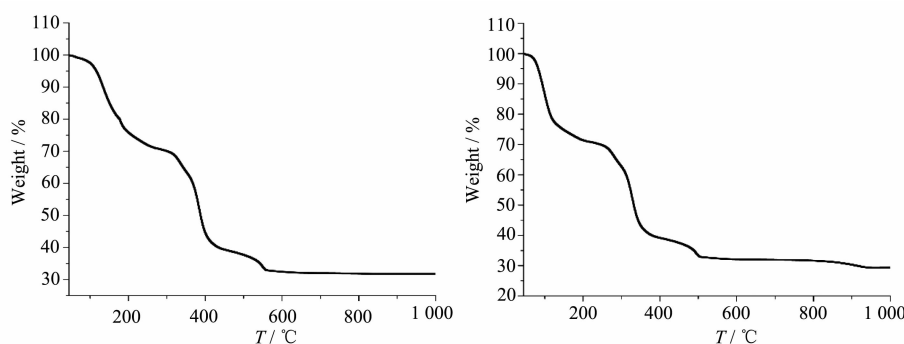

Fig.3　TGA curves of polymers **1**(a) and **2**(b)

the χ_mT begin to decrease slowly, and the decrease in the range of 300~25 K could be attributed to the single ion behavior of Co^{2+}. But the χ_mT more rapidly reduces below 25 K, then reaches a minimum value of 4.46 $cm^3 \cdot mol^{-1} \cdot K$ at 2 K. Combined with the decrease in the χ_mT value when cooling, this result indicates the presence of weak antiferromagnetic interactions in polymer **1**[22]. At 300K, the magnetic moment (μ_{eff}) of cobalt(Ⅱ), which is determined by the equation $\mu_{eff} = 2.828\ (\chi_mT)^{1/2}$, reaches the peak value of $8.74\mu_B$. This value is slightly higher than that expected for an isolated divalent high-spin Co(Ⅱ) system with $\mu_{eff} = 3.87\mu_B$.

As shown in Fig.4b, the molar magnetic susceptibility χ_m of polymer **2** increases gradually as the temperature lowers, and more rapidly increases below 25 K, then reaches a maximum value of 0.48 $cm^3 \cdot mol^{-1}$ at 2 K. It can be seen from the χ_mT curve that the χ_mT value is 3.76 $cm^3 \cdot mol^{-1} \cdot K$ at 300 K, which is equal to the theoretical value of the high-spin binuclear Ni^{2+}. As the decrease of temperature, the χ_mT decrease slowly, and the decrease in the range of 300~25 K could be attributed to the single ion behavior of Ni^{2+}. But there is more rapidly reduction for χ_mT below 25 K, then it reaches a minimum value of 0.96 $cm^3 \cdot mol^{-1} \cdot K$ at 2 K. At 300 K, the magnetic moment (μ_{eff}) of nickel(Ⅱ) reaches the peak value of $5.48\mu_B$. This value is slightly higher than that expected for an isolated divalent high-spin Ni(Ⅱ) system with $\mu_{eff} = 2.83\mu_B$. From magnetic data of the polymers, it is clear that AF coupling mainly occurs between intrachain metal ions.
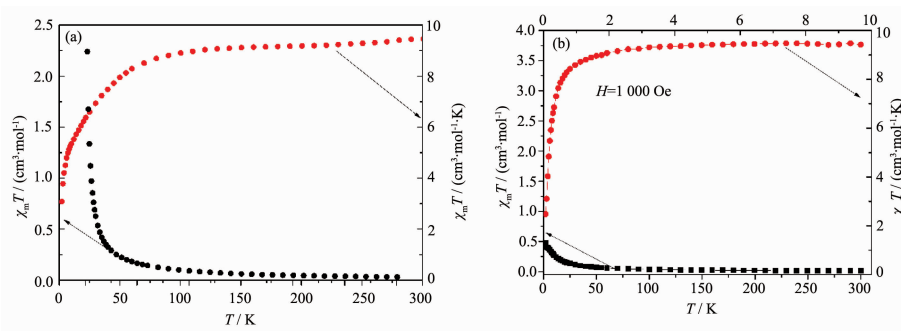

Fig.4　Plots of χ_m and χ_mT vs T of polymers **1**(a) and **2**(b)

3　Conclusions

In summary, two coordination polymers based on pyridine-2,4,6-tricarboxylic acid had been synthesized and characterized. X-ray diffraction study reveals that the polymers **1~2** are isostructural and have two-dimensional network structure. The magnetic measurement reveals the pyridine-2,4,6-tricarboxylic acid as bridge ligand can mediate the antiferromagnetic (AF) coupling interaction between magnetic centers.

References:

[1] Rumberger E M, Shah S J, Beedle C C, et al. *Inorg. Chem.*, **2005,44**:2742-2752

[2] Rinehart J D, Long J R. *Chem. Sci.*, **2011,2**:2078-2085

[3] Meihaus K R, Long J R. *Dalton Trans.*, **2015,44**:2517-2528

[4] Zhang S H, Zhang Y D, Zou H H, et al. *Inorg. Chim. Acta*, **2013,396**:119-125

[5] Zhang S H, Huang Q P, Zhang H Y, et al. *J. Coord. Chem.*, **2014,69**:3155-3166

[6] Wang J H, Zhang S H, Wang W, et al. *J. Cluster Sci.*, **2015, 26**:1129-1142.

[7] Huang X R, Yang L, Zhou Y J, et al. *J. Cluster Sci.*, **2015, 26**:2033-2042

[8] Limas N G, Manz T A. *RSC Adv.*, **2016,6**:45727-45747

[9] Liddle S T, van Slageren J. *Chem. Soc. Rev.*, **2015,44**:6655-6669

[10]Aubin S M J, Wemple M W, Adams D M, et al. *J. Am. Chem. Soc.*, **1996,118**:7746-7754

[11]LI Huan(李欢), CHEN Yun-Zhou(陈云舟), WANG Yan-Jun (王艳君), et al. *Chinese J. Inorg. Chem.*(无机化学学报), **2016,32**:2198-2204

[12]Miyasaka H, Yamashita M. *Dalton Trans*., **2007**,**36**:399-406

[13]Liao B L, Li S X, Guo J J, et al. *Russ. J. Coord. Chem.*, **2016**,**42**:285-291

[14]LIAO Bei-Ling(廖蓓玲), LI Shi-Xiong(李石雄), YIN Xiu-Ju (银秀菊), et al. *Chinese J. Inorg. Chem.*(无机化学学报), **2016**,**32**:1255-1260

[15]Lu J Y. *Coord. Chem. Rev.*, **2003**,**246**:327-347

[16]Zhang L Y, Zhang J P, Lin Y Y, et al. *Cryst. Growth Des.*, **2006**,**6**:1684-1689

[17]Gao H L, Yi L, Zhao B, et al. *Inorg. Chem.*, **2006**,**45**:481-483

[18]Li C J, Peng M X, Leng J D, et al. *CrystEngComm*, **2008**, **10**:1645-1652

[19]Sheldrick G M. *Acta Crystallogr. Sect. A*, **2008**,A**64**:112-122

[20]Bourhis L J, Dolomanov O V, Gildea R J, et al. *Acta Crystallogr. Sect. A*, **2015**,A**71**:59-75

[21]LI Shi-Xiong(李石雄), LIAO Bei-Ling(廖蓓玲), LUO Pei (罗培), et al. *Chinese J. Inorg. Chem.*(无机化学学报), **2015**,**31**:291-296

[22]Jia L H, Li R Y, Duan J M, et al. *Inorg. Chem.*, **2011**,**50**: 144-154